

# Pore alterations of the endothelial lining of rat fenestrated intestinal capillaries exposed to acute stress

Taishi Aosa<sup>1</sup>, Seiichi Chiba<sup>1</sup>, Hirokazu Kitamura<sup>1</sup>, Keisuke Ina<sup>1</sup>, Shuji Tatsukawa<sup>1</sup>, Chinatsu Moriwaki<sup>1</sup>, Huixing Wei<sup>1</sup>, Koro Gotoh<sup>2</sup>, Takayuki Masaki<sup>2</sup>, Tetsuya Kakuma<sup>2</sup>, Hiroataka Shibata<sup>2</sup> and Yoshihisa Fujikura<sup>1</sup>

<sup>1</sup>Department of Molecular Anatomy, Faculty of Medicine and <sup>2</sup>Department of Endocrinology, Metabolism, Rheumatology and Nephrology, Oita University, Hasama-machi, Yufu, Oita, Japan

**Summary.** Stress-induced inflammatory responses in the portal system are characterized by elevations in serum concentrations of interleukin-6 (IL-6) and endotoxins such as lipopolysaccharides (LPS). LPS translocation from the intestinal to the capillary lumen occurs via LPS endocytosis by the capillary endothelium. Because the capillary endothelium of the small intestinal submucosa is fenestrated, we determined the role of pore modifications within the fenestrated endothelium in relaying inflammatory stress responses in the portal vein. We evaluated changes in the diameter and density of endothelial pores of the lamina propria of intestinal villi induced by continuous light (CL) exposure for 48 h and the correlation between these changes and serum IL-6 concentration in the portal vein in a rat model. We found significant increases in both the pore diameter and density, accompanied by a significant increase in portal IL-6 concentration; these changes were significantly attenuated by pretreatment with propranolol, a beta adrenergic receptor antagonist. In contrast, intravenous noradrenaline administration mimicked CL-induced modifications of the diameter and density of pores and the elevation of portal vein IL-6 concentration. These findings suggested that stress-induced inflammatory responses in the portal system may be a part of the modifications of the endothelial pores triggered by sympathetic activation.

**Key words:** Capillary pore, Fenestrated capillary, Stress, interleukin-6, Intestine

## Introduction

Stress affects physiological functions in subjects and results in homeostatic disturbances. Stressors include factors resulting in internal or external environmental changes in emotions, sociological interactions, thermal regulation, energy balance, and metabolism (Selye, 1946; Fadda et al., 1991; Wan et al., 2003; Overton and Williams, 2004; Vere et al., 2009). Although modern life enables us to live and work more comfortably with adequate lighting facilitating work at night, long working hours can trigger stress-mediated disturbances such as hypertension and metabolic dysfunction. In this context, continuous light (CL) exposure has been shown to act as a stressor to the homeostatic regulation through the activation of the central sympathetic nervous system (Nakagawa and Okumura, 2010; Fonken et al., 2013). This stress-induced pathway is associated with thermogenesis of the brown adipose tissue (Cypess et al., 2009) and proinflammatory responses in the hepatic portal system (Takaki et al., 1994; Yagi et al., 2002). In particular, several groups showed that the serum concentrations of proinflammatory factors such as lipopolysaccharides (LPS), fragments of the outer membrane of gram-negative bacteria (Akira et al., 2006), and interleukin-6 (IL-6, a proinflammatory cytokine) were significantly higher in the portal vein than in the systemic veins following sympathetic activation via immobilization stress or electric foot shock (Takaki et

al., 1994; Huang et al., 1997; Yagi et al., 2002). In previous reports, LPS translocation from the intestinal lumen to the lamina propria of intestinal villi, observed with the development of pathology (Akira et al., 2006), were suggested to be involved in the surge of proinflammatory cytokines in intestinal and hepatic disorders (Tomita et al., 2004; Keita et al., 2010). These inflammatory responses to stress occurring in the hepatic portal system appear to be triggered by the influx of LPS from the intestinal lumen to the portal vein (Beutler, 2000; Beutler et al., 2003). However, there are few studies investigating mechanisms underlying LPS translocation from the intestinal lumen to the portal vein, in particular, through the endothelium, except for endocytosis (Akira et al., 2006).

The endothelial pores of the fenestrated portal system capillaries regulate the permeability of substances (Ishimura et al., 1978; Ohtani and Ohtani, 2000; Bendayan, 2002). Potential modifications of the pores of these fenestrated capillaries may serve as gateways for the translocation of proinflammatory substances from the intestinal lumen to the portal vein, as suggested by previous reports (Takaki et al., 1994; Huang et al., 1997; Yagi et al., 2002).

In this study, we focused on the ultrastructure of endothelial pores of the fenestrated capillaries and their roles in changes in stress conditions, such as increased serum IL-6 concentrations in response to CL exposure that mimics modern life stress conditions. Furthermore, we utilized adrenergic agents to determine the role of sympathetic nervous system in this process.

## Materials and methods

### Animals

Adult male Wistar rats weighing approximately 300 g were used for all studies. Animals were housed individually in a soundproof room illuminated daily from 07:00 to 19:00 [12-h light (150–200 lux) or dark (0 lux) cycle] and maintained at  $21 \pm 2^\circ\text{C}$  and  $55 \pm 5\%$  humidity. The animals were fed standard rat chow (Clea rat chow, Fukuoka, Japan) and managed to minimize suffering. All procedures were conducted according to the Oita University guidelines based on the National Institutes of Health guide for the care and use of laboratory animals and were approved by the Animal Care Committee of Oita University (M015004).

### Chemicals

Propranolol hydrochloride solution (Sigma Chemical, MO, USA), an adrenergic beta receptor blocker with a molecular weight of 295.8, was freshly prepared by dissolving in water. Noradrenaline solution (L-norepinephrine hydrochloride; Sigma Chemical, MO, USA), an adrenergic receptor agonist with a molecular weight of 169.18, was freshly prepared by dissolving in saline. Five percent isoflurane (Abbott Japan, Tokyo,

Japan) for the induction and 2% for the conservation was used for inhalation anesthesia.

### Apparatus

The following devices were used in this study: a rectal thermometer for rat rectal temperature (RT) measurement (Small Animal Warmer & Thermometer BWT-100; BRC, Nagoya, Japan), a sphygmomanometer for blood pressure measurement (BP98A; Softron, Tokyo, Japan), an inhalation anesthesia apparatus (NS-AN-10 and NT-10; Neuroscience, Tokyo, Japan), an ultra-microtome (LKB 2088 Ultratome V; LKB, Bromma, Sweden), a metal coating device (Ion Sputter; Hitachi, Tokyo, Japan), an osmium tetra-oxide ( $\text{OsO}_4$ ) coater device with Au (HPC-1S, CVD; Ibaraki, Japan), a lyophilizer (VFD-21; Ibaraki, Japan), a transmission electron microscope (TEM; H-7650; Hitachi, Tokyo, Japan), and a scanning electron microscope (SEM; S-4800; Hitachi, Tokyo, Japan).

### TEM

Tissues were fixed in 50% Karnovsky's fixative (Karnovsky, 1961) for 10 min at  $4^\circ\text{C}$ , rinsed with 0.1 M cacodylate buffer (pH 7.4), and post-fixed in 2%  $\text{OsO}_4$  (0.1 M cacodylate buffer with 1% potassium ferrocyanide) for 2 h at  $4^\circ\text{C}$ . The specimens were dehydrated in an ascending ethanol wash series and embedded in epoxy resin. Ultrathin sections were cut using an ultra-microtome, mounted on copper grids, and stained with methanolic uranyl acetate and lead citrate. Ultrathin sections were evaluated using TEM with an accelerating voltage of 80 kV (Ina et al., 2011).

### SEM

Tissues were fixed in 50% Karnovsky's fixative (Karnovsky, 1961) for 10 min at  $4^\circ\text{C}$ , rinsed with 0.1 M cacodylate buffer (pH 7.4), and immersed in 20% and 40% dimethylsulfoxide (DMSO; Wako, Osaka, Japan) in 0.1 M cacodylate buffer for 60 min each. Samples from the lamina propria of the small intestinal mucosal membranes were frozen with liquid nitrogen in a vacuum bottle, and each block was broken into two cubes, 1 mm on each side, using a razor blade. The fractured pieces were immediately replaced in 40% DMSO and thawed at room temperature. Further, they were rinsed in 0.1 M cacodylate buffer until DMSO was completely removed and fixed in 50% Karnovsky's fixative (Karnovsky, 1961). The specimens were rinsed in 0.1 M cacodylate buffer for 1 h at  $4^\circ\text{C}$  and fixed with 1%  $\text{OsO}_4$  in 0.1 M cacodylate buffer for 1 h. The specimens were made conductive to staining by treating with 1% tannic acid (MERCK, Germany) for 1 h and immersing in 1%  $\text{OsO}_4$  for 1 h. The samples were dehydrated through a graded ethanol series, transferred to t-butyl alcohol (Wako, Osaka, Japan), and freeze-dried in a lyophilizer. After the fractured surfaces were

## Ultrastructure of capillary pores

checked under a dissecting microscope, the dried specimens were mounted on aluminum stubs with silver paste. The specimens were then coated using metal coating and OsO<sub>4</sub> coating devices and observed using SEM at an accelerating voltage of 10 kV (Koga et al., 2012).

### Imaging analysis of the fenestrated endothelial pores

We determined changes in the fenestrated endothelial pores of lamina propria from the small intestinal mucosal membranes, a prominent site for fenestrated endothelia (Stan et al., 2012). The fenestrated endothelial pores were evaluated for diameter and density by TEM image analysis using an automated imaging analysis software (iTEM; Olympus Soft Imaging Solutions, Münster, Germany) (Almubrad and Akhtar, 2011). The diameter of a pore was represented by the length of the fenestrated endothelial diaphragm, and the density of the pores was determined by quantifying the number of pores normalized to the observed field length (Stan et al., 2012). The diameter and lineal density values and ratio of the number of pores to the length of the delineated fenestrated endothelial surface were evaluated and averaged. The evaluations were conducted for a minimum of four areas for each sample, with a minimum of 30 pores in each area analyzed to determine average pore diameter.

### Measurement of urine and serum catecholamine levels

Urine adrenaline and noradrenaline levels were measured by high-performance liquid chromatography (HPLC; L-6000; Hitachi, Tokyo, Japan), as described in detail previously (Honda, 1983). To prevent contamination of urine, 0.5 ml of 6N hydrochloride was prepared beforehand, and the urine samples were collected with a metabolic cage (CL-0304; Clea Japan, Tokyo, Japan). Urine sampling times were 7:00 for Post 12h to 19:00 for Post 24-h collections.

### Enzyme-linked immunosorbent assay

After rats were deeply anesthetized by isoflurane, blood was collected from the portal and right ventricular (RV) veins for sera collection, and a commercially available enzyme-linked immunosorbent assay (ELISA) kit was used to measure IL-6 (Gen-Probe Diaclone SAS, Besançon, France). All reference standards for IL-6 and serum samples were tested in duplicates, and the absorbance was measured at a wavelength of 540 nm.

### Experimental protocol

Continuous light exposure with beta blocker administration

CL exposure with 150-200 lux illumination from a distance of 40-85 cm initiated at 19:00 for 24 h was used

as a stressor for rats. CL exposure stress was created by replacing a normal dark cycle once with a light cycle; lighting time was from 19:00 (Pre 0 h) to 07:00 (Post 12 h). The animals were housed in either the light/dark (LD) or light/light (LL) condition, and half of the animals in each group randomly received either propranolol (2 mg/kg) or water. Thus, rats were randomly placed into one of the four groups (n=8/group): control (LD) rats without propranolol [Group 1 (-/-)], rats under continuous light exposure (LL) without propranolol [Group 2 (-/+)], control rats (LD) with propranolol [Group 3 (+/-)], and rats under continuous light exposure (LL) with propranolol [Group 4 (+/+)]. Propranolol was dissolved in water, and its concentration was adjusted to the water consumed during the dark cycle to ensure correct dosage. Briefly, the average water consumption in rats, approximately 14 ml/100 g of body weight during the dark cycle, was set as the amount of water-propranolol solution. Each rat was ascertained to have consumed water or water-propranolol solution between 19:00 and 07:00, as determined at the end of the CL exposure session. Rectal temperature (RT) and systolic and diastolic blood pressure (SBP and DBP, respectively) were measured every 12 h, once at 07:00 and 19:00. Urine adrenaline and noradrenaline levels were measured every 12 h using urine samples collected at 7:00 (Post 12 h) and 19:00 (Post 24 h).

At the end of experiments, rats were deeply anesthetized by isoflurane, and blood was collected from the right ventricular (RV) and portal veins for serum analysis. The left ventricles were perfused with 50% Karnovsky's fixative solution for TEM and SEM image analysis of the fenestrated endothelial pores. Rats were not used in more than one experiment throughout the study.

Intravenous noradrenaline injection with beta blocker administration

Rats were equally divided into four groups (n=4/group) to determine the dose-response effects of intravenous (iv) noradrenaline on fenestrated endothelial structure. Treatment groups received noradrenaline at doses of 2 pg/kg, 2 ng/kg, or 2 μg/kg, whereas the control group received iv saline injections. Blood was drawn from the tail veins at 09:00, and all rats were deeply anesthetized by isoflurane and perfused through the left ventricle with 50% Karnovsky's fixative at 11:00 for the analysis of pore structure using the imaging software iTEM. Small intestinal samples were collected for image analysis of the fenestrated endothelial pores. Based on the results, the optimal dose was determined to be 2 μg/kg of noradrenaline for time course studies to further analyze pore properties. Rats were divided into eleven groups (n=4/group) to determine time-dependent effects of 2 μg/kg iv noradrenaline administered via the tail vein at 09:00; at indicated times, animals were deeply anesthetized by isoflurane and perfused through

the left ventricle using 50% Karnovsky's fixative for pore structural analysis by TEM. Rats were divided into groups: rats exactly before iv injection of noradrenaline at time point 0 and rats treated as described above for 5, 15, 30, 60, 90, 120, 180, 240, 300, and 360 min after iv injections of noradrenaline (n=2/time point). Small intestinal samples were collected for image analysis of the fenestrated endothelial pores.

Based on the results of these two studies, the response time of 2 h and the optimal dose of 2 µg/kg noradrenaline were used for further pore structural analyses. Rats were equally divided into four groups (n=8/group): rats administered iv saline with peroral water [Group 1 (-/-)], rats administered iv noradrenaline with peroral water [Group 2 (-/+)], rats administered iv saline with peroral propranolol [Group 3 (+/-)], and rats administered iv noradrenaline with peroral propranolol [Group 4 (+/+)]. Oral administration of 2 mg/kg propranolol or an equivalent volume of water was performed with a disposable feeding needle (Feeding Needles 5206; Fuchigami, Kyoto, Japan). Animals first received either propranolol or water at 08:30 and received iv noradrenaline or an equivalent volume of saline (100 µl/kg) to the tail vein at 09:00. At 11:00, all animals were processed for the evaluation of the following: 1) SBP and DBP, 2) serum adrenaline and noradrenaline levels from the RV, 3) serum IL-6 concentrations of the RV and portal veins, and 4) the structural properties of the small intestinal fenestrated endothelial pores, as described above. Rats were not used in more than one experiment in our study.

### Statistical analysis

The data were presented as the means ± standard deviation (SD). Continuous variables, determined with normal distribution by the Shapiro-Wilk test of normality, were compared by the analysis of variance (ANOVA) using JMP software (version 11; SAS, Cary, NC, USA). The dose-response of the fenestrated endothelial pore diameter to noradrenaline was evaluated by linear regression analysis. Statistical significance was set at P<0.05.

## Results

### Stress responses induced by extended light exposure

Table 1 shows the correlation between stress responses in rats that were exposed to CL and/or received propranolol. First, CL exposure for 12 h significantly increased urine noradrenaline concentration, SBP, and DBP in Group 2 compared with Group 1. In addition, urine adrenaline concentration and RT were increased in both Groups 2 and 4 compared with Group 1. Further, these CL exposure-mediated significant changes in SBP, DBP, and RT detected in Group 2 animals were alleviated by propranolol pretreatment in animals in Group 4.

Further, we evaluated the effect of CL exposure on endothelial pore ultrastructure. As observed in representative TEM and SEM images in Fig. 1, CL exposure modified the appearance of vascular endothelium of the

**Table 1.** Changes in stress-associated responses to continuous light exposure and beta blocker administration.

Urine collection from	Group 1 (-/-) Mean ± SD	Group 2 (-/+) Mean ± SD	Group 3 (+/-) Mean ± SD	Group 4 (+/+) Mean ± SD
7:00 (Post 12h) to 19:00 (Post 24h)				
Noradrenaline (µg/l)	538.1±93.22	667.2±73.75*	615.9±54.90	620.3±75.53
Adrenaline (µg/l)	26.1±5.44	38.7±3.87*	33.2±5.42	39.5±9.48*
Systolic blood pressure (mmHg)				
Pre 12 h at 07:00	112.1±8.27	115.3±5.96	113.1±9.58	113.3±8.88
Pre 0 h at 19:00	119.8±8.53	121.7±5.59	121.7±5.96	118.7±10.08
Post 12 h at 07:00	114.5±7.40	130.3±9.01**	117.7±2.06††	118.1±5.12††
Post 24 h at 19:00	119.8±9.51	124.3±7.52	115.3±15.87†	114.4±9.23†
Diastolic blood pressure (mmHg)				
Pre 12 h at 07:00	80.7±10.64	81.1±12.59	78.2±14.50	77.7±9.14
Pre 0 h at 19:00	88.8±5.06	90.1±8.67	90.7±12.20	88.4±13.69
Post 12 h at 07:00	80.0±12.60	91.5±7.25*	79.1±10.71†	82.5±10.78†
Post 24 h at 19:00	88.2±9.81	88.5±14.47	75.3±14.35*†	83.3±13.0
Rectal temperature (°C)				
Pre 12 h at 07:00	37.0±0.28	37.0±0.21	36.8±0.15	37.0±0.27
Pre 0 h at 19:00	37.6±0.20	37.6±0.16	37.6±0.27	37.6±0.40
Post 12 h at 07:00	36.9±0.22	37.8±0.17**	37.0±0.30††	37.4±0.17*†
Post 24 h at 19:00	37.4±0.25	37.5±0.13	37.3±0.18	37.4±0.13

All parameters were measured every 12 h for two consecutive days. Animals were individually housed in either Light/Dark (control, LD) or Light/Light (stress, LL) conditions, and half of the animals in each group randomly received either propranolol or water. Pre 12h: 12 h before the start of stress, Pre 0h: at 0 h, Post 12h: 12 h after the initiation of stress, Post 24h: 24 h after the initiation of stress. Group 1: propranolol-/stress-, Group 2: propranolol-/stress+, Group 3: propranolol+/ stress-, Group 4: propranolol+/ stress+. \*P<0.05, \*\*P<0.01, vs. Group 1 (-/-), ANOVA. †P<0.05, ††P<0.01, vs. Group 2 (-/+), ANOVA.



### Ultrastructure of capillary pores

small intestinal mucosal membranes; increases in the diameter and density of the endothelial pores were observed in Group 2 in response to CL exposure (Fig. 1B,B',b) compared with the controls in Group 1 (Fig. 1A,A',a). In addition, these changes were blunted by pretreatment with propranolol as observed in Group 4 (Fig. 1D,D',d). These observations were confirmed by measurements of the diameter and density of the endothelial pores. Table 2A includes the quantitative changes in these characteristics of the endothelial pores. Group 3 that was treated with propranolol, but not exposed to CL, did not show any significant modifications of the diameter or density of endothelial pores.

Further, we determined the association between CL exposure and changes in serum IL-6 levels. The assessment of portal vein and RV samples revealed serum IL-6 levels were higher in the portal vein than the RV in all groups, irrespective of CL exposure (Table 2B). In addition, the augmentation of the endothelial pore properties with CL exposure in the absence of propranolol pretreatment, as shown in Table 1 and Fig. 1, was accompanied by significant increases in serum IL-6 concentrations in both the RV and portal vein in

Group 2 (Table 2B) compared with Group 1. Finally, serum IL-6 level of the portal vein was significantly higher than that of the RV in only Group 2.

#### Dose- and time-dependent effects of noradrenaline on endothelial pore dilatation

Fig. 2A shows the dose response of pore diameter to increasing doses of iv noradrenaline. There was a statistically significant and linear increase in the pore diameter with 2.0  $\mu\text{g}/\text{kg}$  noradrenaline (diameter=4.0668056 $\pm$ 0.0081451; \*log,  $r=0.22$ ,  $P<0.05$ ). As shown in Fig. 2B,C, there were time-dependent significant changes in the density and diameter of endothelial pores with 2  $\mu\text{g}/\text{kg}$  iv noradrenaline treatment for approximately 120 min after the injections. The increase in pore density was uniphasic (Fig. 2B), whereas the increase in pore diameter was biphasic (Fig. 2C).

#### Noradrenaline-mediated stress responses

Table 3 summarizes the changes in noradrenaline-mediated stress responses with propranolol pretreatment. Thirty minutes after 2 mg/kg peroral

**Table 2.** The pore dynamics and cytokine levels in response to continuous light exposure.

A. Measurement of pore ultrastructure				
Fenestrated capillary endothelial pores	Group 1 (-/-) Mean $\pm$ SD	Group 2 (-/+) Mean $\pm$ SD	Group 3 (+/-) Mean $\pm$ SD	Group 4 (++) Mean $\pm$ SD
Diameter (nm)	46.4 $\pm$ 9.16	51.9 $\pm$ 9.57*	46.1 $\pm$ 8.05†	45.5 $\pm$ 8.25†
Density (count/ $\mu\text{m}$ )	39.0 $\pm$ 6.29	54.8 $\pm$ 9.58*	41.5 $\pm$ 4.91†	42.9 $\pm$ 10.63†
B. Circulatory dynamics of IL-6 levels				
IL-6 levels (pg/ml)	Group 1 (-/-) Mean $\pm$ SD	Group 2 (-/+) Mean $\pm$ SD	Group 3 (+/-) Mean $\pm$ SD	Group 4 (++) Mean $\pm$ SD
RV	86.3 $\pm$ 16.90	173.8 $\pm$ 79.40*	105.3 $\pm$ 56.75†	141.3 $\pm$ 57.13
Portal vein	134.3 $\pm$ 38.15	256.9 $\pm$ 128.11*§	147.8 $\pm$ 50.47†	199.0 $\pm$ 36.02

Diameter, diameter of the fenestrated capillary endothelial pore; Density, ratio of the number of pores to the length of observed area; RV, right ventricle; Group 1, propranolol-/ stress-; Group 2, propranolol-/stress+; Group 3, propranolol+/ stress-; Group 4, propranolol+/ stress+. \* $P<0.05$ , \*\* $P<0.01$  vs. Group 1 (-/-), ANOVA. †  $P<0.05$  vs. Group 2 (-/+), ANOVA. § $P<0.05$  vs. Group 2 (-/+ ) RV.

**Table 3.** Stress responses to intravenous noradrenaline (2.0  $\mu\text{g}/\text{kg}$ ) administration with beta blocker pretreatment.

	Group 1 (-/-) Mean $\pm$ SD	Group 2 (-/+) Mean $\pm$ SD	Group 3 (+/-) Mean $\pm$ SD	Group 4 (++) Mean $\pm$ SD
Rectal temperature ( $^{\circ}\text{C}$ )	37.0 $\pm$ 0.16	37.5 $\pm$ 0.31*	36.4 $\pm$ 0.21†	37.3 $\pm$ 0.39
Systolic blood pressure (mmHg)	115.8 $\pm$ 6.15	132.4 $\pm$ 4.36*	110.3 $\pm$ 9.12†	123.9 $\pm$ 3.09†
Diastolic blood pressure (mmHg)	85.4 $\pm$ 6.69	103.1 $\pm$ 12.95*	77.8 $\pm$ 17.07†	95.2 $\pm$ 3.86†
Catecholamine level in serum				
Noradrenaline (pg/l)	1652.4 $\pm$ 526.42	2933.1 $\pm$ 589.28**	2019.0 $\pm$ 662.14	2636.4 $\pm$ 476.6**
Adrenaline (pg/l)	7556.6 $\pm$ 2198.47	11211.6 $\pm$ 1664.21**	9387.3 $\pm$ 3155.54†	11862.4 $\pm$ 1912.65**

Comparisons of the catecholamine mean ( $\pm$  SEM) values after noradrenaline intravenous injection versus vehicle administration. Group 1, propranolol-/noradrenaline-; Group 2, propranolol-/noradrenaline+; Group 3, propranolol+/ noradrenaline -; Group 4, propranolol+/ noradrenaline +. \* $P<0.05$ , \*\* $P<0.01$  vs. Group 1 (-/-), ANOVA. †  $P<0.05$  vs. Group 2 (-/+), ANOVA.

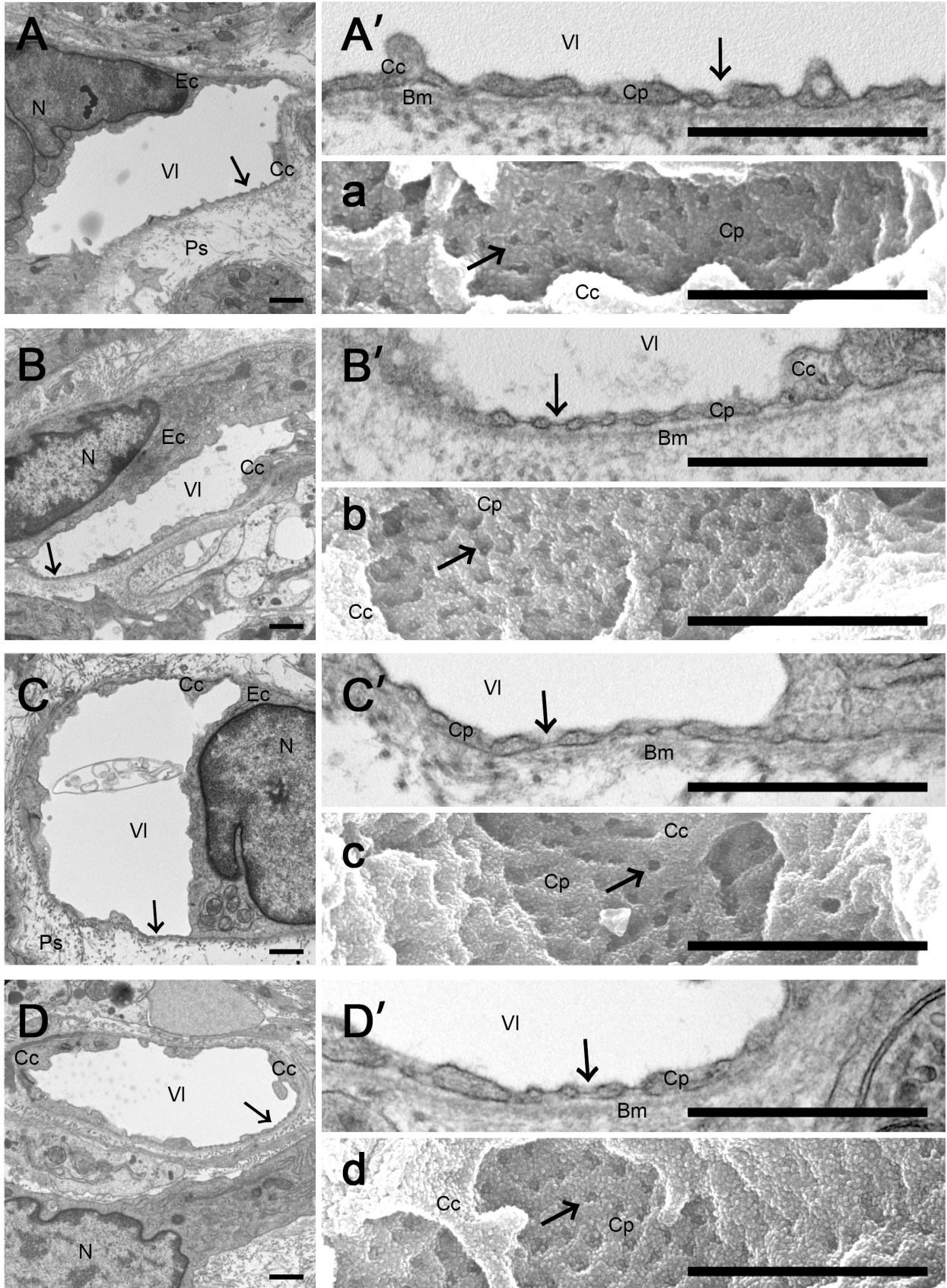


**Fig. 1.** The effect of continuous light exposure stress on fenestrated capillaries. Ultrastructure of the pore (arrow) and pore-related cells by TEM (A-D, A'-D') and SEM (a-d). Group 1, propranolol-/stress- (A, A', a); Group 2, propranolol-/stress+ (B, B', b); Group 3, propranolol+/stress- (C, C', c); Group 4, propranolol+/stress+ (D, D', d). The arrow indicates the endothelial pore location. Bm, basal membrane; Cc, cytoplasmic crests; Cp, cytoplasm; Ec, endothelial cell; N, nucleus; Ps, perivascular space; VI, vascular lumen. Scale bar: 1  $\mu$ m.

Ultrastructure of capillary pores

propranolol or vehicle, 2 µg/kg noradrenaline or 100 µl/kg saline was injected into the tail veins, as described in the Methods section. Noradrenaline significantly increased the RT in Group 2 compared with Group 1 and resulted in significant increases in SBP, DBP, and serum noradrenaline and adrenaline levels in both Group 2 and Group 4, compared with Group 1. These noradrenaline-mediated changes in SBP and DBP in Group 2 were significantly decreased in the propranolol-treated animals in Group 4. Group 3 animals that received propranolol, but not noradrenaline injection did not show any significant changes in RT, SBP, or DBP compared to controls in Group 1; however, serum adrenaline and noradrenaline levels tended to increase with propranolol in Group 3 animals.

As shown in Fig. 3, noradrenaline administration modified the appearance of vascular endothelium of the small intestinal mucosal membranes as observed by TEM and SEM. Augmentations in the diameter and density of the endothelial pores, indicated by arrows, were observed in Group 2 specimens (Fig. 3B,B',b, Table 3), compared to Group 1 controls (Fig. 3A,A',a); these changes were in parallel to the significant increases detected in serum catecholamine levels. In addition, noradrenaline-mediated increases in the diameter and density were blunted by propranolol pretreatment, as observed in Group 4 specimens (Fig. 3D,D',d), which were comparable with the diameter and density of specimens from Group 3 animals that received only propranolol (Fig. 3C,C',c). These observations were

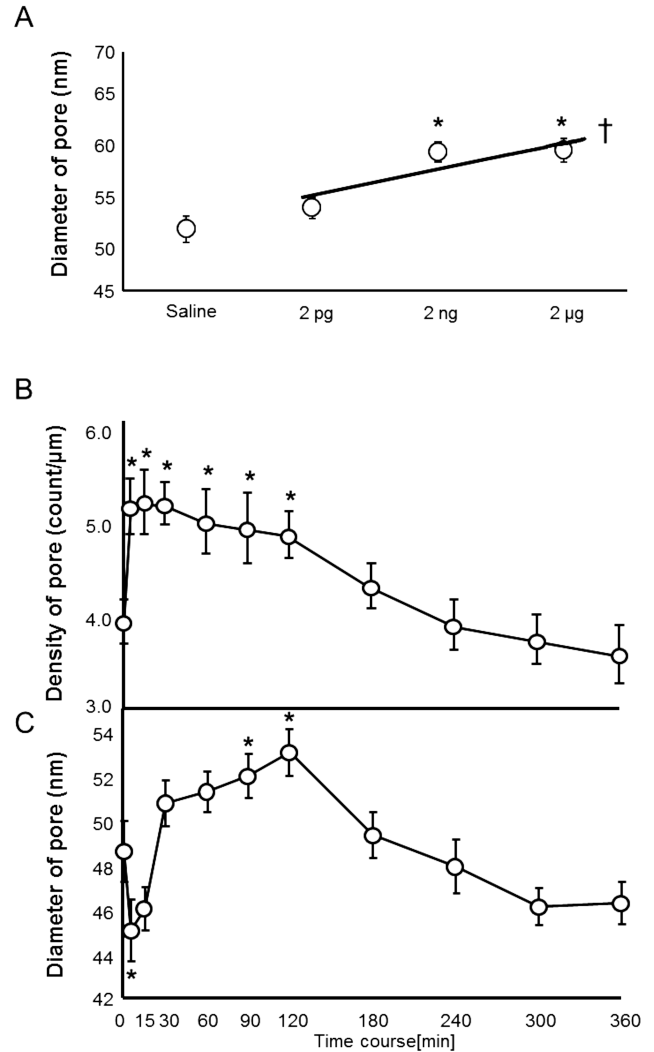


**Fig. 2.** Dose- and time-dependent responses of fenestrated capillary endothelial pores. **A.** Dose response to intravenous noradrenaline injection. Data represented as the mean and the error bars represent standard error of means (SEM). \*P<0.05 vs. 2 pg/kg and saline. The linear relationship ( $Y=4.0668056 + 0.0081451 \cdot \log$ ,  $r=0.22$ ) was confirmed (†P<0.05). **B and C.** Time-dependent response to intravenous 2µg/kg noradrenaline injection. Data represented as the mean and the error bars represent SEM. \*P<0.05 vs. 0 min.

**Table 4.** Cytokine levels in circulation and pore dynamics in response to intravenous noradrenaline administration.

A. Measurement of pore ultrastructure				
Fenestrated capillary endothelial pores	Group 1 (-/-) Mean ± SD	Group 2 (-/+) Mean ± SD	Group 3 (+/-) Mean ± SD	Group 4 (+/+) Mean ± SD
Diameter (nm)	49.9±8.95	58.9±10.30*	51.3±9.19†	55.0±10.42†
Density (count/µm)	51.7±7.28	62.2±6.08*	52.8±6.32†	57.6±7.47†
B. Circulatory dynamics of IL-6 levels				
IL-6 levels (pg/ml)	Group 1 (-/-) Mean ± SD	Group 2 (-/+) Mean ± SD	Group 3 (+/-) Mean ± SD	Group 4 (+/+) Mean ± SD
RV	82.0±22.67	112.1±28.35	79.7±16.23	105.4±48.96
Portal vein	189.1±51.90§	309.3±153.33*§	193.7±63.44†§	191.7±91.82†§

Diameter, diameter of the fenestrated capillary endothelial cell pore; Density, ratio of the number of pores to the length of the area observed; RV, right ventricle. Group 1, propranolol-/noradrenaline-; Group 2, propranolol-/noradrenaline+; Group 3, propranolol+/noradrenaline-; Group 4, propranolol+/noradrenaline+. \*P<0.05, \*\*P<0.01 vs. Group 1 (-/-), ANOVA. †P<0.05 vs. Group 2 (-/+), ANOVA. §P<0.05 vs. RV.



## Ultrastructure of capillary pores

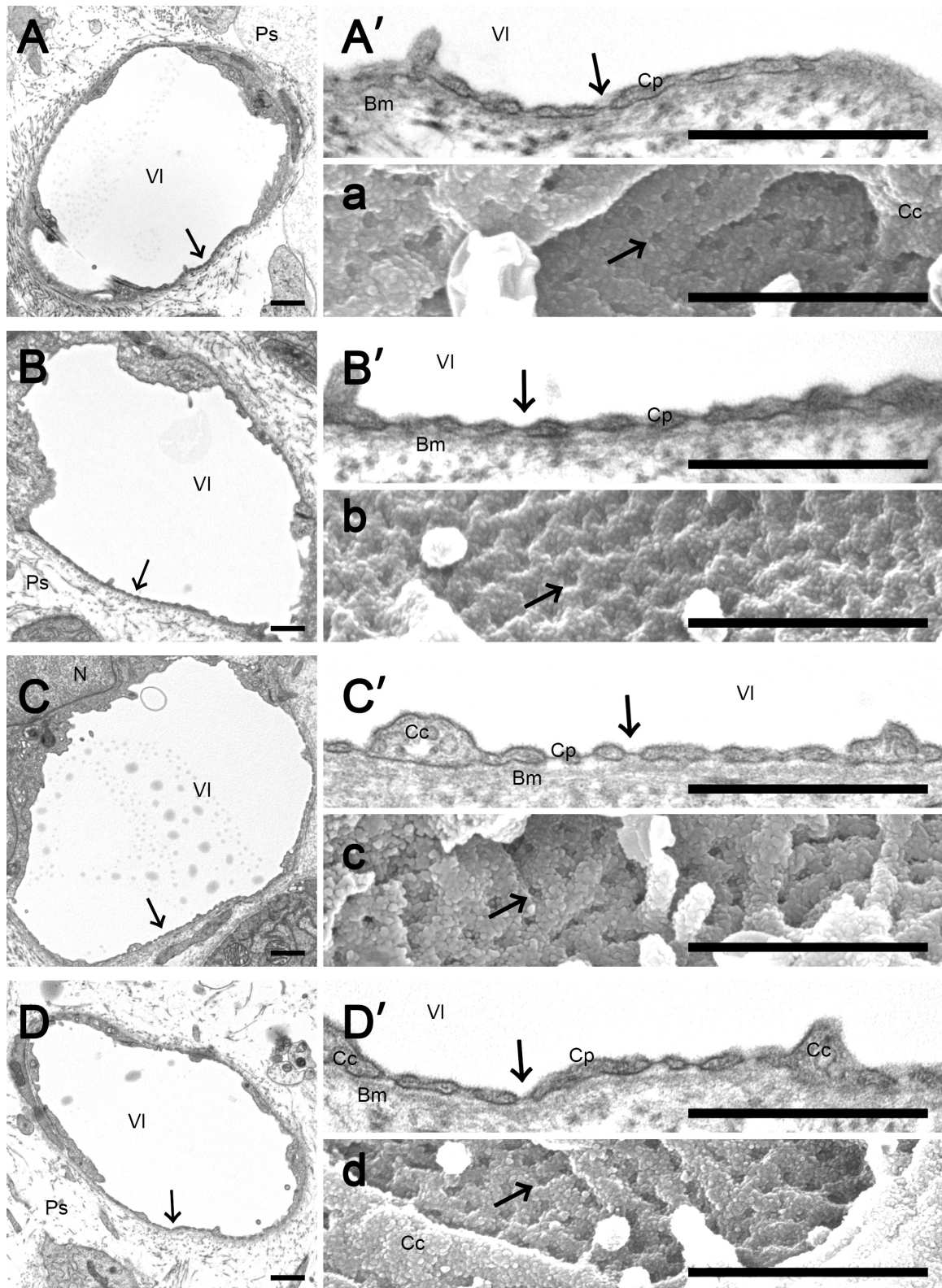


**Fig. 3.** Changes in ultrastructure of fenestrated capillaries induced by intravenous noradrenaline injection (2.0  $\mu\text{g}/\text{kg}$ ) with or without pretreatment with propranolol (2 mg/kg). Ultrastructure of the pore (arrow) and pore-related cells by TEM (A-D, A'-D') and SEM (a-d) images. Group 1, propranolol/noradrenaline- (A, A', a); Group 2, propranolol/adrenaline+ (B, B', b); Group 3, propranolol+/adrenaline- (C, C', c); Group 4, propranolol+/adrenaline+ (D, D', d). The arrow indicates the endothelial pore location. Bm, basal membrane; Cc, cytoplasmic crests; Cp, cytoplasm; Ec, endothelial cell; N, nucleus; Ps, perivascular space; VI, vascular lumen. Scale bar: 1  $\mu\text{m}$ .



confirmed by quantitative measurements of the diameter and density of endothelial pores, as summarized in Table 4A. The significant increases in pore diameter and density with noradrenaline in Group 2 specimens were significantly alleviated by propranolol pretreatment as observed in Group 4 specimens. Group 3, which received propranolol, but not noradrenaline, did not show any significant modifications of the endothelial pore diameter and density compared with Group 1, apart from the significant increments in the diameter and the density compared with that in Group 2.

Further, we assessed changes in serum IL-6 levels associated with changes in endothelial pore structure. As observed in Table 4B, increases in the endothelial pore diameter and density with noradrenaline alone were followed by a significant increase in serum IL-6 concentrations in Group 2 animals, particularly from the portal vein (Table 4B). The comparison of serum IL-6 concentrations between the RV and portal veins revealed that serum IL-6 increases observed in the portal vein was significantly higher than that observed in the RV in groups. This increment in the portal serum IL-6 concentration showed variation; the most significant increment was detected in Group 2, which was significantly diminished in Groups 3 and 4; however, no significant variation was seen among RV serum IL-6 concentrations across all groups.

## Discussion

In this study, we showed the effects of changes in the catecholaminergic system on the microvascular endothelial pores in the lamina propria of small intestinal mucosal membranes. The endothelial pore diameter and density were significantly increased by CL exposure, which is considered a mild stressor, through beta adrenergic regulation (Tables 1-2, Fig. 1). Direct administration of an optimal dose of noradrenaline (Fig. 2) to the cardiovascular system mimicked the physiological responses to CL exposure that were attenuated by blocking beta adrenergic receptors by propranolol (Tables 3-4, Fig. 3). Mild stressors were reported to increase serum IL-6 levels in the portal vein through sympathetic nervous system activation, accompanied by elevations in RT, SBP and DBP (Takaki et al., 1994; Huang et al., 1997; Yagi et al., 2002). Our results showing changes in urine catecholamine excretion, SBP, DBP, RT, and serum IL-6 levels in response to either CL exposure or iv noradrenaline administration are in agreement with these earlier studies. Further, we showed that these responses could be significantly alleviated by pretreatment with propranolol, a beta receptor antagonist (Tables 1-4). As predicted by previous reports (Takaki et al., 1994; Huang et al., 1997; Yagi et al., 2002), the increases in endothelial pore diameter and density correlated with CL exposure-induced physiological responses, as indicated by increased serum IL-6 concentrations in the portal vein (Tables 2,4). The attenuation of changes in endothelial

pore diameter and density by beta adrenergic receptor block (Table 2) suggests that the sympathetic nervous system may be participating in CL exposure-mediated regulation of endothelial pore dynamics in our model; this was confirmed by direct noradrenaline administration to the systemic circulation using an optimal dose of 2  $\mu\text{g}/\text{kg}$  based on the initial dose-response studies. Intravenous noradrenaline significantly augmented endothelial pore diameter and density, which were significantly suppressed by adrenergic beta receptor block (Table 4), similar to those observed in the CL exposure paradigm (Table 2). This beta adrenergic regulation of endothelial pore dynamics was reflected in serum IL-6 changes, particularly in the portal vein (Table 4). Collectively, these results indicate that potent activation of the sympathetic nervous system may dilate the endothelial pores, allowing for enhanced translocation of proinflammatory substances such as LPS from the intestinal lumen into the portal vein, as previously reported (Takaki et al., 1994; Yagi et al., 2002). The augmentation of endothelial pores in the presence of stress, which could be regulated by beta adrenergic receptors, reveals a novel mechanism for the transmission of stress signals from the small intestine to the portal vein and liver, the site of IL-6 biosynthesis in response to stress conditions. The confirmation of direct translocation of proinflammatory substances via augmented endothelial pores and the potential mechanisms underlying this dynamic regulation of microvascular endothelial pores in the lamina propria of small intestinal mucosal membranes will be investigated in future studies.

Increases in serum IL-6 levels in response to a variety of stressors, such as immobilization and electrical foot shock in animals, are well documented (Takaki et al., 1994; Liao et al., 1995; Huang et al., 1997; Yagi et al., 2002). Other triggers for increased IL-6 induction in the portal vein include stress-aggravated translocation of intestinal endotoxins (Wigg et al., 2001; Tomita et al., 2004; Keita et al., 2010; Samak et al., 2010), epinephrine-mediated induction from isolated Kupffer cells (Liao et al., 1995), norepinephrine-mediated induction from isolated hepatocytes (Jung et al., 2000), cold stress in the liver via sympathetic nervous system (Yildirim and Yurekli, 2010), heat stress (Hagiwara et al., 2011), fructose feeding (Sivakumar and Anuradha, 2011), oxidative stress (AlSaid et al., 2015), and non-alcoholic fatty liver disease (Wigg et al., 2001). Our observation of elevated serum IL-6 in the portal vein that was induced by CL exposure might be due to the activation of the sympathetic nervous system, as previously reported (Craft et al., 1985; Chiarenza et al., 1989; Simko et al., 2014). Alternatively, direct catecholaminergic effects in Kupffer cells and hepatocytes may be driving IL-6 induction in our model, as suggested before (Owman et al., 1982; Briaud et al., 2004). Our novel findings of dynamic augmentation of the endothelial pores that were associated with sympathetic activation may be contributing to IL-6

induction in the hepatic portal area, as suggested in previous reports (Takaki et al., 1994; Liao et al., 1995; Huang et al., 1997; Yagi et al., 2002).

Although the exact regulatory mechanism underlying the dynamic augmentation of endothelial pores remains unexplained in this study, previous studies showed several functions that are modulated by catecholamines: the function of actin-binding proteins of the endothelium regulating the permeability of the endothelial barrier in an ATP-dependent manner (Flint et al., 2011; García-Ponce et al., 2015) and the expression and function of PV1 of the endothelial pore diaphragms, a gatekeeper that regulates the permeability of the endothelium (Stan, 2004; Stan et al., 2012). In future studies, we will determine the role of endothelial pore dynamics in conditions of sympathicotonia such as cold exposure, hypoglycemia, and obesity.

*Acknowledgements.* We thank Yukari Goto, the secretary for the Molecular Anatomy lectures, for supporting this study.

*Conflict of interest.* Authors declare that they received no support of any form and there is no conflict of interest.

## References

- Akira S., Uematsu S. and Takeuchi O. (2006). Pathogen recognition and innate immunity. *Cell* 124, 783-801.
- Almubrad T. and Akhtar S. (2011). Structure of corneal layers, collagen fibrils, and proteoglycans of tree shrew cornea. *Mol. Vis.* 17, 2283-2291.
- AlSaid M., Mothana R., Raish M., Al-Sohaibani M., Al-Yahya M., Ahmad A., Al-Dosari M. and Rafatullah S. (2015). Evaluation of the effectiveness of piper cubeba extract in the amelioration of CCl<sub>4</sub>-induced liver injuries and oxidative damage in the rodent model. *Biomed. Res. Int.* 2015, 359358.
- Bendayan M. (2002). Morphological and cytochemical aspects of capillary permeability. *Microsc. Res. Tech.* 57, 327-349.
- Beutler B. (2000). Endotoxin, toll-like receptor 4, and the afferent limb of innate immunity. *Curr. Opin. Microbiol.* 3, 23-28.
- Beutler B., Hoebe K., Du X. and Ulevitch R.J. (2003). How we detect microbes and respond to them: the Toll-like receptors and their transducers. *J. Leukoc. Biol.* 74, 479-485.
- Briaud S.A., Zhang B.L. and Sannajust F. (2004). Continuous light exposure and sympathectomy suppress circadian rhythm of blood pressure in rats. *J. Cardiovasc. Pharmacol. Ther.* 9, 97-105.
- Chiarenza A.P., Sanz E.G., Vermouth N.T., Aoki A. and Bellavia S.L. (1989). Effects of continuous light on rat parotid gland structure and reactivity. *Anat. Embryol. (Berl.)* 179, 497-501.
- Craft C.M., Morgan W.W., Jones D.J. and Reiter R.J. (1985). Hamster and rat pineal gland beta-adrenoceptor characterization with iodocyanopindolol and the effect of decreased catecholamine synthesis on the receptor. *J. Pineal. Res.* 2, 51-66.
- Cypess A.M., Lehman S., Williams G., Tal I., Rodman D., Goldfine A.B., Kuo F.C., Palmer E.L., Tseng Y.H., Doria A., Kolodny G.M. and Kahn C.R. (2009). Identification and importance of brown adipose tissue in adult humans. *Engl. J. Med.* 360, 1509-1517.
- Fadda P., Tortorella A. and Fratta W. (1991). Sleep deprivation decreases mu and delta opioid receptor binding in the rat limbic system. *Neurosci. Lett.* 129, 315-317.
- Flint M.S., Budiu R.A., Teng P.N., Sun M., Stolz D.B., Lang M., Hood B.L., Vlad A.M. and Conrads T.P. (2011). Restraint stress and stress hormones significantly impact T lymphocyte migration and function through specific alterations of the actin cytoskeleton. *Brain Behav. Immun.* 25, 1187-1196.
- Fonken L.K., Lieberman R.A., Weil Z.M. and Nelson R.J. (2013). Dim light at night exaggerates weight gain and inflammation associated with a high-fat diet in male mice. *Endocrinology* 154, 3817-3825.
- García-Ponce A., Citalán-Madrid A.F., Velázquez-Avila M., Vargas-Robles H. and Schnoor M. (2015). The role of actin-binding proteins in the control of endothelial barrier integrity. *Thromb. Haemost.* 113, 20-36.
- Hagiwara S., Iwasaka H., Shingu C., Matsumoto S., Uchida T., Nishida T., Mizunaga S., Saikawa T. and Noguchi T. (2011). Danaparoid sodium attenuates the effects of heat stress. *J. Surg. Res.* 171, 762-768.
- Honda S., Takahashi M., Araki Y. and Kakehi K. (1983). Postcolumn derivatization of catecholamines with 2-cyanoacetamide for fluorimetric monitoring in high-performance liquid chromatography. *J. Chromatogr.* 274, 45-52.
- Huang Q.H., Takaki A. and Arimura A. (1997). Central noradrenergic system modulates plasma interleukin-6 production by peripheral interleukin-1. *Am. J. Physiol.* 273, 731-738.
- Ina K., Kitamura H., Tatsukawa S. and Fujikura Y. (2011). Significance of  $\alpha$ -SMA in myofibroblasts emerging in renal tubulointerstitial fibrosis. *Histol. Histopathol.* 26, 855-866.
- Ishimura K., Okamoto H. and Fujita H. (1978). Freeze-etching images of capillary endothelial pores in the liver, thyroid and adrenal of the mouse. *Arch. Histol. Jpn.* 41, 187-193.
- Jung B.D., Kimura K., Kitamura H., Makondo K., Okita K., Kawasaki M. and Saito M. (2000). Norepinephrine stimulates interleukin-6 mRNA expression in primary cultured rat hepatocytes. *J. Biochem.* 127, 205-209.
- Karnovsky M.J. (1961). Simple methods for "staining with lead" at high pH in electron microscopy. *J. Biophys. Biochem. Cytol.* 11, 729-732.
- Keita A.V., Söderholm J.D. and Ericson A.C. (2010). Stress-induced barrier disruption of rat follicle-associated epithelium involves corticotropin-releasing hormone, acetylcholine, substance P, and mast cells. *Neurogastroenterol. Motil.* 22, 770-778.
- Koga D., Nakajima M. and Ushiki T. (2012). A useful method for observing intracellular structures of free and cultured cells by scanning electron microscopy. *J. Electron Microsc.* 61, 105-111.
- Liao J., Keiser J.A., Scales W.E., Kunkel S.L. and Kluger M.J. (1995). Role of epinephrine in TNF and IL-6 production from isolated perfused rat liver. *Am. J. Physiol.* 268, 896-901.
- Nakagawa H. and Okumura N. (2010). Coordinated regulation of circadian rhythms and homeostasis by the suprachiasmatic nucleus. *Proc. Jpn. Acad. Ser. B Phys. Biol. Sci.* 86, 391-409.
- Ohtani O. and Ohtani Y. (2000). A corrosion casting/scanning electron microscope method that simultaneously demonstrates clear outlines of endothelial cells and three-dimensional vascular organization. *Arch. Histol. Cytol.* 63, 425-429.
- Overton J.M. and Williams T.D. (2004). Behavioral and physiologic responses to caloric restriction in mice. *Physiol. Behav.* 81, 749-759.
- Owman C., Edvinsson L., Lindvall M. and Sjöberg N.O. (1982). Influence of external light conditions on norepinephrine levels in organs innervated by sympathetic nerves from different levels. *Brain Res. Bull.* 9, 777-779.

*Ultrastructure of capillary pores*

- Samak G., Suzuki T., Bhargava A. and Rao R.K. (2010). c-Jun NH2-terminal kinase-2 mediates osmotic stress-induced tight junction disruption in the intestinal epithelium. *Am. J. Physiol. Gastrointest. Liver Physiol.* 299, 572-584.
- Selye H. (1946). The general adaptation syndrome and the diseases of adaptation. *J. Allergy* 17, 231, 358.
- Simko F., Pechanova O., Repova Bednarova K., Krajcovicova K., Celec P., Kamodyova N., Zorad S., Kucharska J., Gvozdjakova A., Adamcova M. and Paulis L. (2014). Hypertension and cardiovascular remodelling in rats exposed to continuous light: protection by ACE-inhibition and melatonin. *Mediators Inflamm.* 2014, 703175.
- Sivakumar A.S. and Anuradha C.V. (2011). Effect of galangin supplementation on oxidative damage and inflammatory changes in fructose-fed rat liver. *Chem. Biol. Interact.* 193, 141-148.
- Stan R.V. (2004). Multiple PV1 dimers reside in the same stomatal or fenestral diaphragm. *Am. J. Physiol. Heart. Circ. Physiol.* 286, 1347-1353.
- Stan R.V., Tse D., Deharvengt S.J., Smits N.C., Xu Y., Luciano M.R., McGarry C.L., Buitendijk M., Nemani K.V., Elgueta R., Kobayashi T., Shipman S.L., Moodie K.L., Daghlian C.P., Ernst P.A., Lee H.K., Suriawinata A.A., Schned A.R., Longnecker D.S., Fiering S.N., Noelle R.J., Gimi B., Shworak N.W. and Carrière C. (2012). The diaphragms of fenestrated endothelia: gatekeepers of vascular permeability and blood composition. *Dev. Cell* 11, 1203-1218.
- Takaki A., Huang Q.H., Somogyvári-Vigh A. and Arimura A. (1994). Immobilization stress may increase plasma interleukin-6 via central and peripheral catecholamines. *Neuroimmunomodulation* 1, 335-342.
- Tomita M., Ohkubo R. and Hayashi M. (2004). Lipopolysaccharide transport system across colonic epithelial cells in normal and infective rat. *Drug Metab. Pharmacokinet.* 19, 33-40.
- Vere C.C., Streba C.T., Streba L.M., Ionescu A.G. and Sima F. (2009). Psychosocial stress and liver disease status. *World J. Gastroenterol.* 15, 2980-2986.
- Wan R., Camandola S. and Mattson M.P. (2003). Intermittent food deprivation improves cardiovascular and neuroendocrine responses to stress in rats. *J. Nutr.* 133, 1921-1929.
- Wigg A.J., Roberts-Thomson I.C., Dymock R.B., McCarthy P.J., Grose R.H. and Cummins AG. (2001). The role of small intestinal bacterial overgrowth, intestinal permeability, endotoxaemia, and tumour necrosis factor alpha in the pathogenesis of non-alcoholic steatohepatitis. *Gut* 48, 206-211.
- Yagi S., Takaki A., Hori T. and Sugimachi K. (2002). Enteric lipopolysaccharide raises plasma IL-6 levels in the hepatoportal vein during non-inflammatory stress in the rat. *Fukuoka Igaku Zasshi* 93, 38-51.
- Yildirim N.C. and Yurekli M. (2010). The effect of adrenomedullin and cold stress on interleukin-6 levels in some rat tissues. *Clin. Exp. Immunol.* 161, 171-175.

Accepted January 5, 2016